INVESTIGATION REPORT ET/IR 637

Greenhouse gas emissions from spontaneous combustion at open cut coal mines: An investigation of air quality modelling and inverse techniques

ACARP Project C11023

by

William Lilley and John N Carras

CSIRO Energy Technology

PMB7, Bangor, NSW, 2234

October 2003

Summary

While spontaneous combustion of coal has been recognised by the Inter-Governmental Panel for Climate Change (IPCC) as a potential source of greenhouse gas emissions, it has been excluded from greenhouse gas inventories as it is considered that there is no acceptable method for estimating the emissions.

In recognition of this, ACARP has carried out two previous projects to explore methods for establishing greenhouse gas emissions from spontaneous combustion. The first project, C8059 (Carras et al, 2000) sought to provide methods, supported by direct measurement, to quantify the emissions. Measurements of emissions from spoil piles, coal rejects and tailings were conducted at 11 mines in the Hunter Valley in NSW and the Bowen Basin in Queensland using a chamber technique. While the project significantly advanced the knowledge of emissions from spontaneous combustion in open cut coal mines, there were practical problems in applying the results to estimate greenhouse gas emissions from operating mines.

The second project funded by ACARP, C9062 (Carras et al, 2002) used airborne infra-red thermography to investigate whether more accurate and cost-effective monitoring of the extent of spontaneous combustion in spoil piles and the associated greenhouse gas emissions could be achieved. The main conclusion drawn by Carras et al (2002) was that airborne infra-red data could be used to monitor the long term behaviour of spoil piles subject to spontaneous combustion. However, due to the complexity of the processes involved in producing heating and its surface manifestation and the associated emissions of greenhouse gases, the emissions estimates were still subject to significant uncertainty.

At the conclusion of projects C8059 and C9062 the focus of the research centred on reducing the uncertainty associated with the emission estimates.

The aim of the current study is to investigate a method for determining the emissions of CO_2 from spontaneous combustion in spoil piles at open cut coal mines, through the use of air quality methods, including modeling and inverse techniques.

The approach used was to model the large sources of CO_2 in the Hunter Valley using a computer based air quality model (TAPM) which has been widely used in air pollution studies in Australia. An investigation of CO_2 sources in the Upper Hunter Valley has shown that spontaneous combustion and power stations can give rise to significant concentrations at ground level. However the impact of the power stations emissions are most pronounced during the day time hours while the impact of the spontaneous combustion emissions are most pronounced during the night time. This is because the former are elevated while the latter are ground level sources. This suggests that concentration measurements should focus on data during the night time period. While the emissions from road traffic and rail are significant their ground level concentration signature is not as pronounced as for the other two major sources.

Consideration of results of the air quality modelling suggests that monitoring sites for the inverse modelling should be sited such that;

- The location point should be sufficiently close to the spontaneous combustion sources to enable a large measurable signal.
- The site should be chosen on the basis of meteorology to best capture the likely CO_2 spontaneous combustion signal
- The sites should be chosen to minimise the influence of other sources.

In order to examine some of the issues that would need to be taken into account in using air quality methods, concentrations were predicted for three chosen locations and examined in greater detail. The predicted concentration time series were used as surrogates for measured data and a simple ratio method used to produce results which highlighted the uncertainties associated with this approach.

In addition to these inherent uncertainties there will also be those due to the non ideal nature of the data and the fact that the air quality model still represents an approximation to reality. Supplementation of the CO_2 concentration data with other micrometeorological data would constrain the data and reduce the uncertainty. In addition concurrent ground based field measurements of CO_2 traverses across the plume coupled with the micrometeorological data and detailed plume modelling would provide the basis for a robust methodology to estimate greenhouse gas emissions from spontaneous combustion.

TABLE OF CONTENTS

1. INTRODUCTION

1.1 Spontaneous combustion and greenhouse gas emissions

While spontaneous combustion of coal has been recognised by the Inter-Governmental Panel for Climate Change (IPCC) as a potential source of greenhouse gas emissions, it has been excluded from greenhouse gas inventories as it is considered that there is no acceptable method for estimating the emissions.

In their study for the Australian Coal Association on greenhouse gas emissions from coal mining, Williams et al. (1998), suggested that up to 25 percent of the total emissions from an open cut coal mine with spontaneous combustion in the spoil may arise from spontaneous combustion and low temperature coal oxidation. While the assessment made by these authors represented the "state of the art" at the time, the estimates were based on very limited data and had large associated uncertainty.

Following on from the work of Williams et al (1998), ACARP has carried out two previous projects to explore methods for establishing greenhouse gas emissions from spontaneous combustion. The first project, C8059 (Carras et al, 2000) sought to provide methods, supported by direct measurement, to quantify the emissions. Measurements of emissions from spoil piles, coal rejects and tailings were conducted at 11 mines in the Hunter Valley in NSW and the Bowen Basin in Queensland using a chamber technique. The results of this work led to the development of emission factors for several broad categories based on the extent of spontaneous combustion present. These were

1. intense spontaneous combustion characterised by smoke and steam, major cracks, surface discolouration and obvious signs of venting;
2. spontaneous combustion with less well pronounced signs, small cracks, surface discolouration and occasional whisps of smoke and steam;
3. no sign of spontaneous combustion.

While Project C8059 significantly advanced the knowledge of emissions from spontaneous combustion in open cut coal mines, there were practical problems in applying the results to estimate greenhouse gas emissions from operating mines. While the chamber technique developed in that project provided direct emission measurements, it was labour intensive and required many measurements to obtain representative values. In addition, it is difficult obtain an objective measure of the extent of spontaneous combustion in spoil piles.

The second project funded by ACARP, C9062 (Carras et al, 2002) investigated the use of a remote sensing technique, airborne infra-red thermography, to investigate whether more accurate and cost-effective monitoring of the extent of spontaneous combustion in spoil piles and the associated greenhouse gas emissions could be achieved. This approach was based on the finding by Carras et al (2000) that an approximate relationship existed between the emission rate of greenhouse gases and the average surface temperature of the spoil pile surface.

The main conclusions drawn by Carras et al (2002) were that airborne infra-red data could be used to monitor the long term behaviour of spoil piles subject to spontaneous combustion. The same data could also be used to estimate greenhouse gas emissions for spontaneous combustion. However, due to the complexity of the processes involved in producing heating and its surface manifestation and the associated emissions of greenhouse gases, the emissions estimates were still subject to significant uncertainty. Nevertheless (and the scatter in the data notwithstanding) over a suitable time period the method could be used to monitor the progress of spontaneous combustion in spoil piles and associated emission of greenhouse gases.

A further approach which has been considered in estimating emissions from spontaneous combustion requires the direct measurement of emission fluxes by mapping out the concentration of GHG as a function of crosswind distance, height above the ground and wind speed, to allow a direct estimate of the emission rate. This technique has been employed previously by Williams et al (1990) and Carras et al (1994, 2002), using an aircraft, to measure

- the fluxes of methane emitted from Sydney, Melbourne and Brisbane
- the volatile organic compounds (VOC) emitted from the Kwinana industrial region and
- the emissions of VOC and nitrogen oxides (NO_x) emitted from Hong Kong.

While this approach is the most direct it requires traverses of the downwind plume at various heights above the ground. However, ground level sources require very low level passes through the plume. While these can be achieved above the sea such traverses are vastly more difficult and dangerous above land. Thus and notwithstanding the appeal of this approach for open cut coal mines, safety issues preclude the use of airborne methods in this manner.

At the conclusion of projects C8059 and C9062 the focus of the research centred on reducing the uncertainty associated with the emission estimates.

A variation of the direct flux measurement approach described above is to traverse a ground based CO_2 detector across the plume and to use knowledge of micrometeorology and plume dispersion to estimate the horizontal and vertical extent of the plume and hence calculate the emission rate. This approach was used by Williams et al (1991) in their estimates of methane fluxes from open-cut coal mines.

In addition to the methods described above to determine area source emissions, another approach that has been gaining widespread use in recent years, particularly with regard to global greenhouse gas emissions, is the use of inverse methods. Inverse methods, as the name implies arise from inverting the normal advection diffusion equation used to describe transport of gases and particles in the atmosphere. For instance, in conventional applications of atmospheric transport models such as air quality models, a source strength and meteorological data are used as input to calculate the concentration of a species at

downwind locations. By contrast, an inverse technique involves back–calculating the strength of an emissions source using a measured concentration time series at one or a number of selected sites.

While there has been considerable work on methods to invert air pollution concentrations in order to obtain estimates of the emission strengths of sources, developing a completely general inversion method is not possible as information is lost as the pollution cloud advects and diffuses in the atmosphere. Other physical information is required to constrain the possible solutions to the equations and yield realistic results. In general, the greater the number of monitors and the 'cleaner' the signal from an individual source the better the solution to the inverse problem. In addition and for the case of CO_2 emissions from spontaneous combustion in the Hunter Valley, the importance of the concentrations from other sources in the Valley such as power stations and the major highway must be taken into account in order to design an appropriate experimental approach to provide greenhouse gas emissions from spontaneous combustion.

The current project developed from these considerations and explores these issues in order to determine the best method for estimating greenhouse gas emissions from spontaneous combustion.

1.2 Objective

The aim of the current study is to investigate a method for determining the emissions of CO_2 from spontaneous combustion in spoil piles at open cut coal mines, through the use of air quality methods, including modeling and inverse techniques.

2. METHODOLOGY

2.1 Inverse modelling techniques

In general, in an Eulerian framework, the concentration downwind of a distributed surface source of emission strength $Q'(x',y',0,t)$ is given by the expression

$$\chi(x,y,z,t) = \int_{x_1}^{x_2}\int_{y_1}^{y_2} Q'(x',y',0,t')k(x,y,z,t,x',y',0,t')dy'dx'$$

where $\chi(x,y,z,t)$ is the downwind concentration and the function $k(x,y,z,t,x',y',0,t')$ contains all the information concerning atmospheric transport, dilution and diffusion. The limits of integration cover the extent of the emission region. In the simple case where the emission rate is constant in space and time the above expression simplifies to

$\chi(x,y,z,t) = Qf(x,y,z,t)$ where Q is the constant emission rate and $f(x,y,z,t) = \int_{x_1}^{x_2}\int_{y_1}^{y_2} k(x,y,z,x',y',0,t)dy'dx'$. The equation can be written in abbreviated form as $\chi_t = Qf_t$, where the subscript 't' indicates the time dependence. In the current work this will be taken to refer to the one hour average value.

If the values of χ_t are available from measurements and the values of the function f_t available from a model, then the $\chi_t's$ can be regressed against the $f_t's$ to obtain Q.

There has been considerable work in the past on methods to invert air pollution concentrations in order to obtain estimates of the emission strengths of sources. However, as indicated above, developing a completely general inversion method is not possible as there is information loss as the pollution cloud advects and diffuses in the atmosphere. Other physical information is required to constrain the solutions to the equations. This may take the form of filtering procedures to choose periods for greater study, or detail about the spatial distribution of the sources. In addition the approach taken in applying inverse methods depends on the scale of the domain over which solutions are sought.

Four examples of inverse modelling which are relevant to the current study and highlight the issues which must be considered are the work of Lehning et al (1994), Mulholland and Sienfeld (1995), Wang and Bentley (2002) and van Aardene et al (2002). Lehning et al (1994) investigated the use of two simple plume dispersion models based on Gaussian and K theory considerations and applied these to back calculate a) the emission strength of a distributed SF_6 release and b) the source characteristics of three artificially created data sets for complex source data. They used an iterative method from Cahine (1970) and Twomey (1977) based on reducing the scaled residuals between the measured data and the values predicted from the model. Lehning et al (1994) found that with a sufficient

number of measuring sites (22 in one case) they could reproduce the detailed form of a complex area source and the total emission rate to a high degree of precision. However, their attempts to reproduce the emission rates of SF_6 from field releases and a limited number of measurements showed some significant scatter for the 1 hour time scales they were considering. For the four individual sets of data the calculated emission rates varied from 17% below the measured value to 34%, 66% and up to a factor of ~3.5 greater than the measured value. However, this is not surprising given the nature of plume behaviour and the short time frame over which the measurements were performed. These uncertainties would be smoothed out for longer period averages.

Seinfeld and Mulholland (1995) presented a general mathematical formulation of the inverse problem and used the techniques to compare measurements of CO at numerous sites within an urban area with air quality model outputs over time periods of days. They developed a Kalman filter based approach and used the results to make spatial and temporal adjustments to CO emission factors within the Californian airshed. The adjustments were performed by comparing observations at 27 sites for a two-day simulation period.

Wang and Bentley (2002) used an inverse method to investigate the total methane emissions from the south-central and southeastern sections of the Australian continent and from Tasmania. They used hourly methane measurements from Cape Grim in Tasmania and suggested that the methane emissions for these regions were overstated by the inventory. Their inversion methods used information on the relative distribution and magnitude of the sources as described in the Australian methane inventory. In order to stabilize their fitting procedure they used an approach based on Bayesian statistics and assumed that the source fluxes could be considered as independent random normal variables. These techniques are powerful, and the solutions generated, robust.

van Aardene et al (2002) used a simpler form of inverse modelling based on wind direction dependencies of SO_2 observations at several sites within Europe to provide a constraint on the inverse problem. They used this approach to pinpoint areas where existing large scale emission inventories were deficient.

In considering the nature and scope of the inverse modelling appropriate for the current study there are a number of factors which must be taken into account. Of major significance are the spatial and temporal scales. For instance Lehning et al (1994) used a simple plume model with spatial scales measured in metres and time scales of hours. Mulholland et al (1995) used a spatial grid 5x5km and time scales of days, while van Ardenne et al (2002) used a spatial grid covering Europe and 24 hour average data for 1 year. Wang and Bentley divide Australia into 8 regions and calculated atmospheric transport on a grid measuring 75kmx75km. While finer time scales and grid sizes provide greater modelling resolution they also increase markedly the computational memory and time required. Also of major significance is the number of monitoring sites and the quality of the data produced from the sites. Errors in the data will introduce errors into the inverse calculations which can be amplified. In general the greater the number of monitors the more constrained the inverse solution will be and the higher the quality of

the results. However, the cost of maintaining monitors in the field is sufficient that there are normally only a small number available.

In addition to the above considerations information such as wind direction dependency can be used to constrain the acceptable solutions. Also of significance in considering the emissions from a small number of sources within a region such as the upper Hunter Valley is the influence of other major emitters of the target pollutant. For the Hunter these include the power stations and the emissions from road and rail transport.

As a result of the above considerations the work in this project was carried out in two stages. The first stage consisted of assessing the major sources of CO_2 in the Hunter Valley and the significance of the emissions from spontaneous combustion on the general CO_2 concentrations in the region. The second stage consisted of exploring the siting of monitoring sites and the quality of the data required, in order to apply local high resolution methods to invert the air quality modeling approach so as to yield greenhouse gas emissions from spontaneous combustion sources.

2.2 Brief description of TAPM

Modelling for the current project was performed for a year using Version 2.0 of the mesoscale atmospheric dispersion model TAPM. CO_2 was modelled in an inert tracer mode using estimated emissions for spontaneous combustion, power station, railway and motor vehicle sources. Details of the general model setup and emission structure are provided below. Results from the model are used to derive a numerical method to estimate an emission flux from a selected spontaneous combustion region within the Hunter Valley.

The Air Pollution Model (TAPM) (Hurley 1998) solves the fundamental fluid dynamics and scalar transport equations to predict meteorology and concentrations for a range of pollutants important for air pollution applications. It consists of coupled prognostic meteorological and air pollution components, eliminating the need to have site-specific meteorological observations except for model validation purposes. Instead, the model predicts the flows important to local-scale air pollution, such as sea breezes and terrain induced flows, using synoptic-scale meteorological analyses as the large-scale background metrological field.

The meteorological component of TAPM is an incompressible, non-hydrostatic, primitive equation system with a terrain-following vertical coordinate for three-dimensional simulations. The model solves the momentum equations for horizontal wind components, the incompressible continuity equation for vertical velocity, and scalar equations for virtual potential temperature and specific humidity of water vapour, cloud water and rain water. The Exner pressure function is split into hydrostatic and non-hydrostatic components, and a Poisson equation is solved for the non-hydrostatic component. Explicit cloud micro-physical processes are included.

The turbulence terms in these equations are determined through solution of equations for turbulence kinetic energy and eddy dissipation rate. These values are then used in a

gradient diffusion representation of the vertical fluxes, including a counter-gradient term for the heat flux. A vegetative canopy and soil scheme is used to model energy partitioning at the surface, while radiative fluxes, both at the surface and at upper levels, are also specified.

The air pollution component of TAPM, used the predicted meteorology and turbulence to predict trace species concentrations in three modules. The Eulerian Grid Module (EGM) solves prognostic equations for concentration and for the cross-correlation of concentration and virtual potential temperature. The Lagrangian Particle Module (LPM) can be used to represent near-source dispersion more accurately, while the Plume Rise Module is used to account for plume momentum and buoyancy effects for point sources. The model also includes gas-phase photochemical reactions based on the Generic Reaction Set (Azzi et al, 1992), and gas- and aqueous-phase chemical reactions for sulfur dioxide and particles. Wet and dry deposition effects are also included although these aspects have not been subjected to validation studies.

2.3 Set-up and application of TAPM Version 2.0

Meteorological fields were generated on a series of nested grids with spacing of 10 km, 3 km and 1 km. All domains were configured with 45 nodes in the easterly, 65 nodes in the northerly directions respectively and 25 nodes in the vertical direction. Vertical layers were concentrated within the planetary boundary layer to better capture local meteorological events. Emissions were calculated on a grid of double density (89 x 129) representing a spacing of 5km, 1.5km and 500 m. Each domain was centered at the Australian Map Grid (AMG) coordinates of 307800 east, 6422620 north as displayed in Figure 1. The outermost grid corresponded to an area measuring 440 x 640 km while the innermost grid measured 44 x 64 km.

Figure 1: TAPM computational domain for 1 km (inner) grid

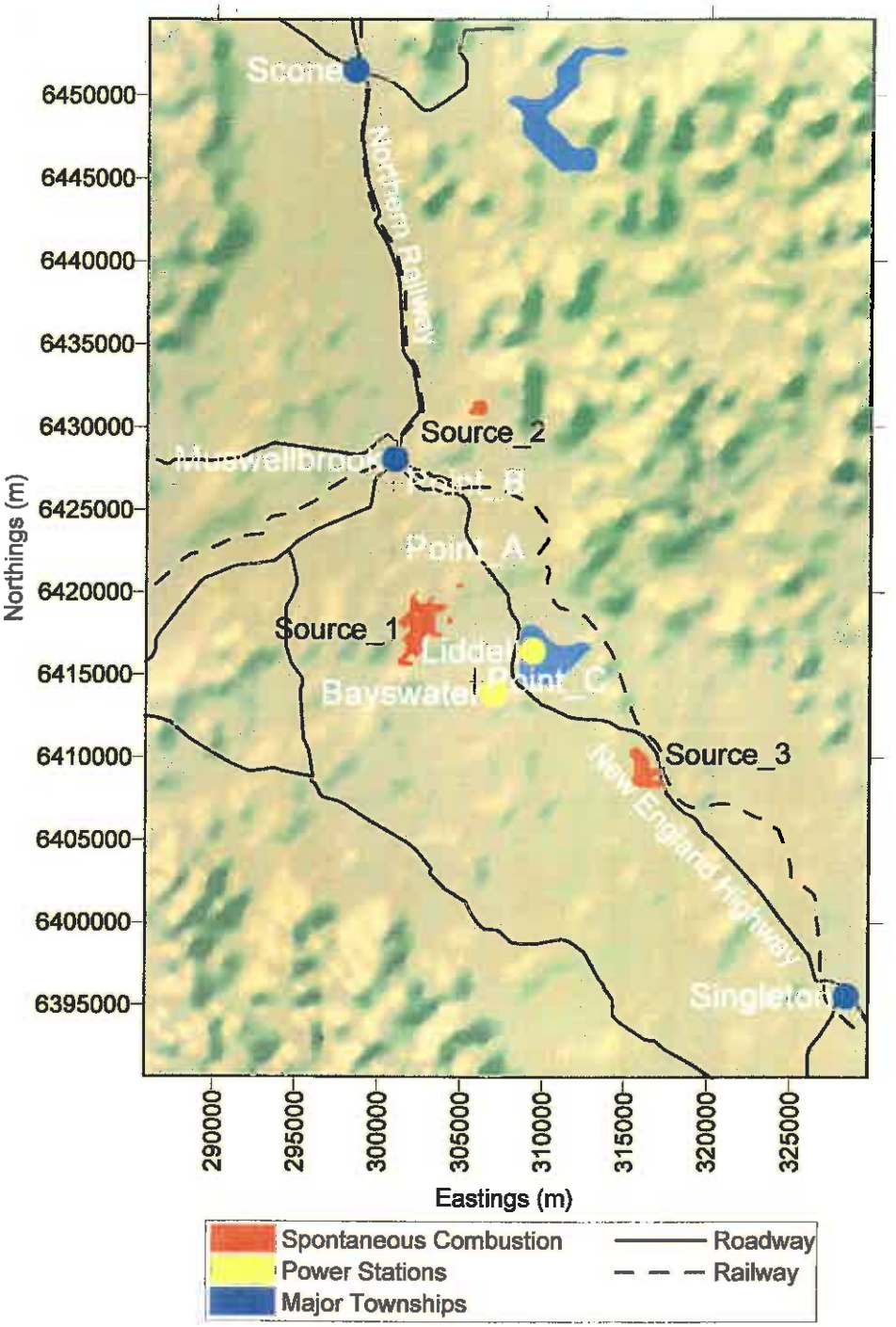

2.4 Emission rates

While estimating the emission rates from spontaneous combustion forms the major aim of the work, there may be other significant sources of CO_2 in the vicinity of open cut coal mines. In the Hunter Valley these include the two large power stations Liddell and Bayswater whose CO_2 plumes are the largest in the region and could easily swamp any possible emissions from spontaneous combustion. As well as those emissions we have also included those from major roads including the New England Highway. Details are as follows;

2.4.1 Spontaneous combustion sources

Three separate scenarios were constructed to investigate CO_2 emissions from the three spontaneous combustion sources displayed in Figure 1.

Initially, three source areas were modelled for a year assuming a spatially and temporally constant emission rate of 100 $kgm^{-2}y^{-1}$. This value is representative of the lower bound limit of CO_2 emission rates measured by Carras et al. (2002). The bounding area of each source group as displayed in Figure 1, were derived from the thermal images of Carras et al (2002). The largest source (Source 1) is situated NW of the Liddell and Bayswater power stations. The smallest source (Source 2) is located NE of Muswellbrook and the final source (Source 3) is sited SE of Liddell and Bayswater power stations near the New England Highway. Emissions were modelled as a collection of individual area sources 250 x 250 meters in size.

In addition to the constant area source scenarios, eight 'hotspot' sensitivity runs were performed for a one month period (February). These calculations were performed by setting the emission rate for selected 250 x 250 m cells within area of Source 1 with a constant emission rate of 3000 $kgm^{-2}y^{-1}$. In this case, the value was chosen to represent the larger value measured by Carras et al. (2000). The number of hotspots used in this study ranged from 1 (e.g. Hotspot_1) to 5 (e.g. Hotspot_4). The centre positions of each cell for the eight hotspot scenarios are displayed with black diamonds in Figure 2.

Figure 2. Hotspot positions

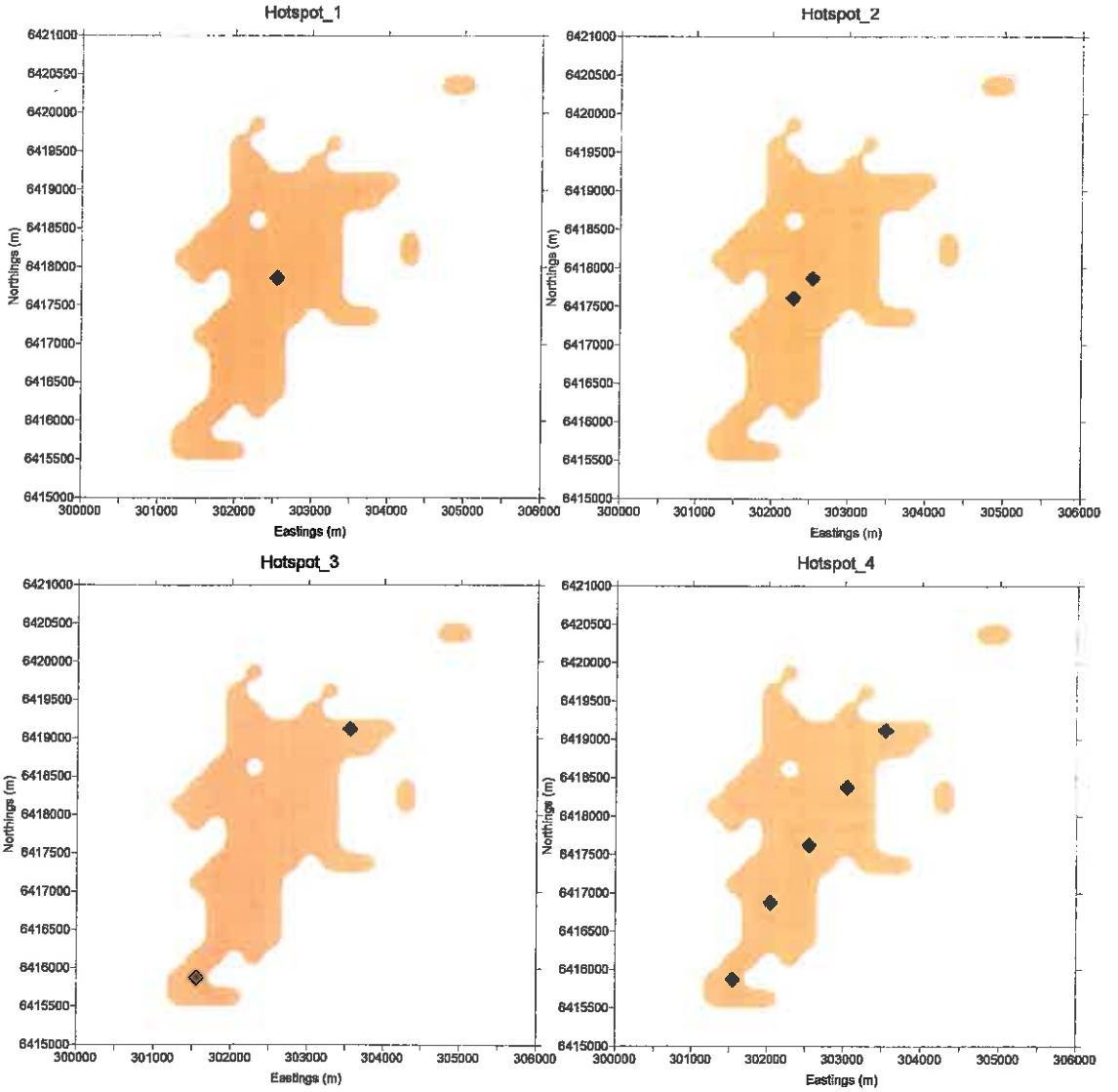

Figure 2 (cont). Hotspot positions

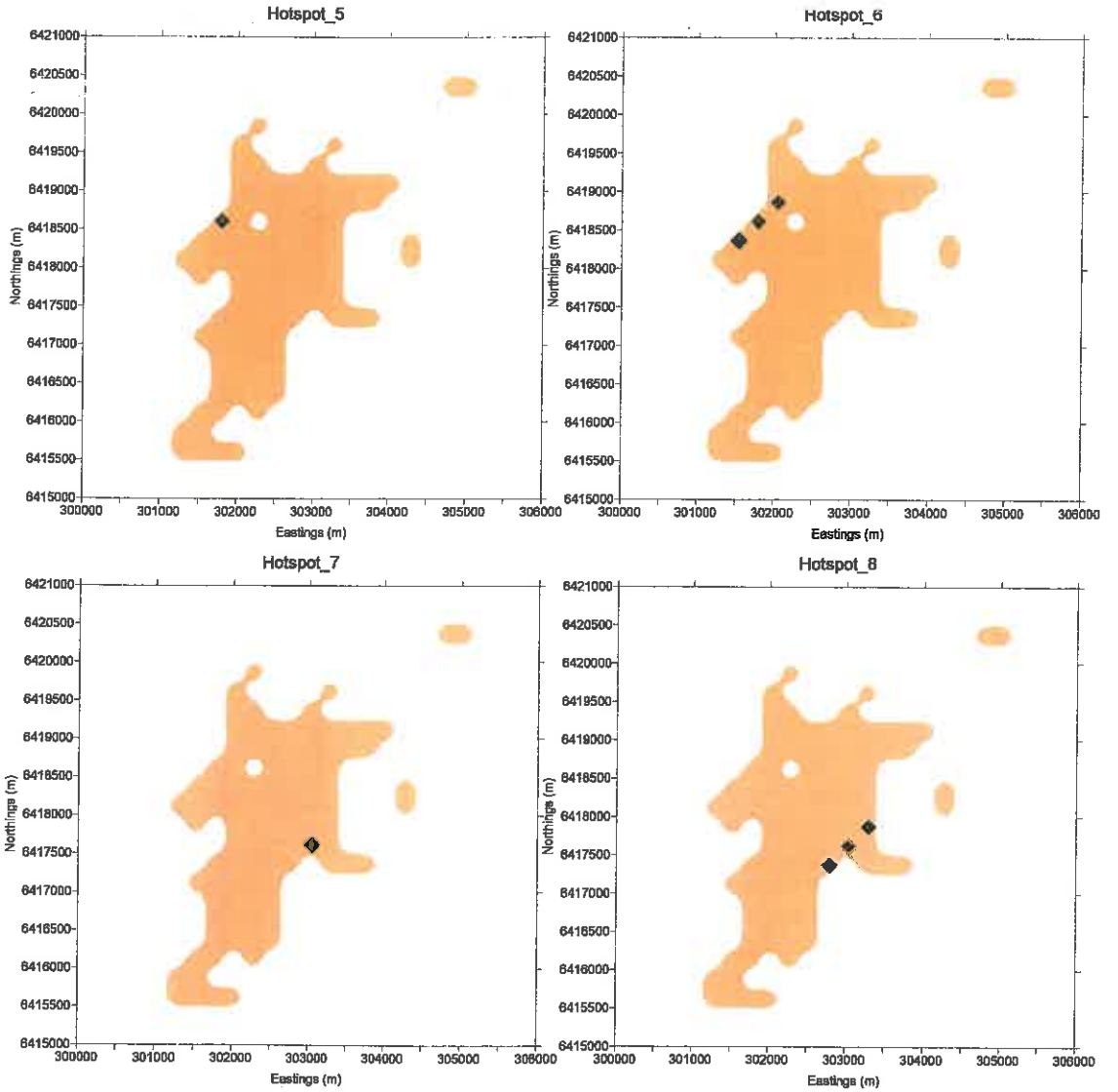

Table 2 provides the normalised (to basecase) total emission rate for Source 1, for each hot spot scenario.

Table 2. Normalised emission rates for hotspot sensitivity runs

Case	Number of standard sources	Number of hotspots	Normalised emission rate
Constant	97	0	1.00
Hotspot_1	96	1	1.30
Hotspot_2	94	3	1.90
Hotspot_3	95	2	1.60
Hotspot_4	92	5	2.50
Hotspot_5	96	1	1.30
Hotspot_6	94	3	1.90
Hotspot_7	96	1	1.30
Hotspot_8	94	3	1.90

Finally, the three sources were again modelled for one full year but with Source 1 emission rates derived from thermal imagery. Source 2 and 3 were again set constant in space and time. Figure 3 provides a spatial representation of the variation in emission magnitude for Source 1. These data were calculated from the emission rate of data obtained by Carras et al (2002). In this case, values ranged between 5 $kgm^{-2}y^{-1}$ and 1265 $kgm^{-2}y^{-1}$ producing an overall normalised source 1 emission rate of 4.25.

Figure 3. Spatial variation in emission intensity from thermal imagery for source 1. (Blue = low, Red = high)

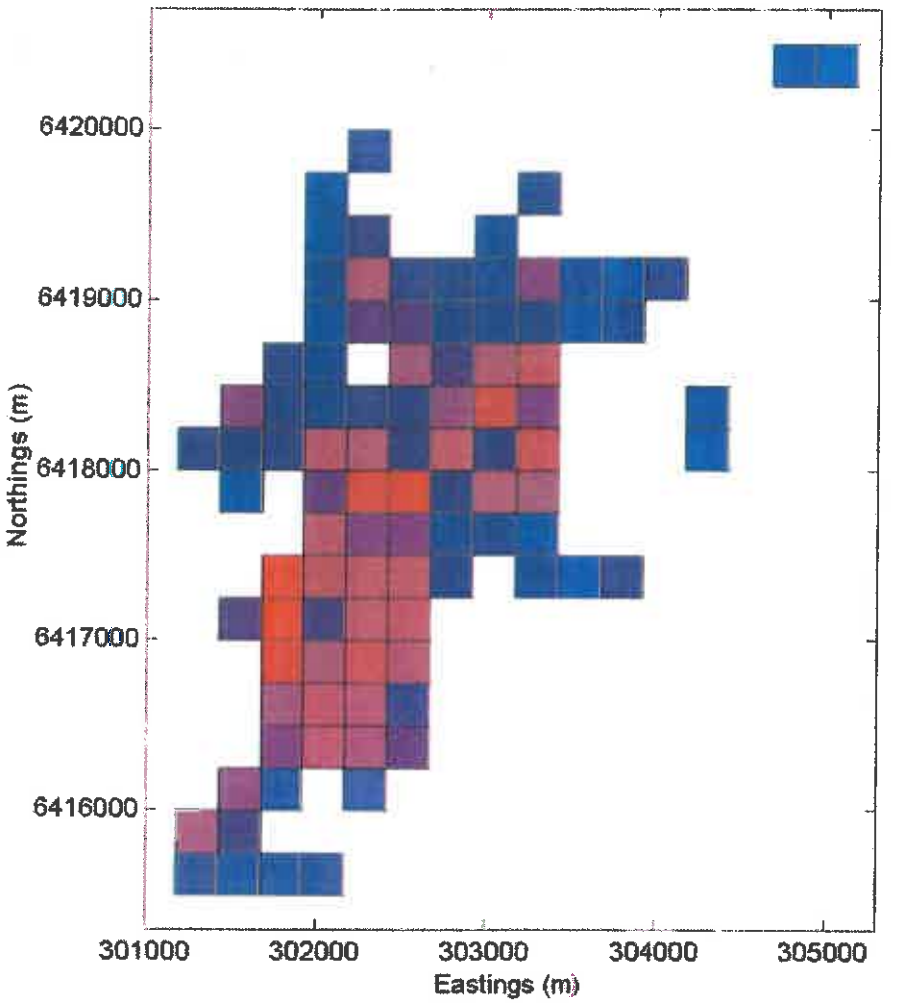

2.4.2 Other sources

In order to provide a guide to the likely contribution of sources other than spontaneous combustion to the CO_2 profile within the inner modeling domain, emissions from power stations, road traffic and locomotives were also modelled with simple diurnal variations.

Emissions from Liddell and Bayswater power stations were modelled in Lagrangian mode whilst all other point sources outside the inner domain were modelled in the default Eulerian mode. Liddell, Bayswater and Eraring power stations were modelled with enhanced buoyancy in accordance with Manins et al., (1992) to accommodate for plume overlap due to the close proximity of multiple stacks. Diurnal profiles were specified for all power stations assuming a generalised artificial 24 hour load profile (Figure 4). Gross average emission factors for each power station were derived from the NGGI (1996), and adjusted for thermal efficiency assuming a NSW average value of 35.2 % (ESAA, 2001).

Figure 4. Generalised load factor for power stations

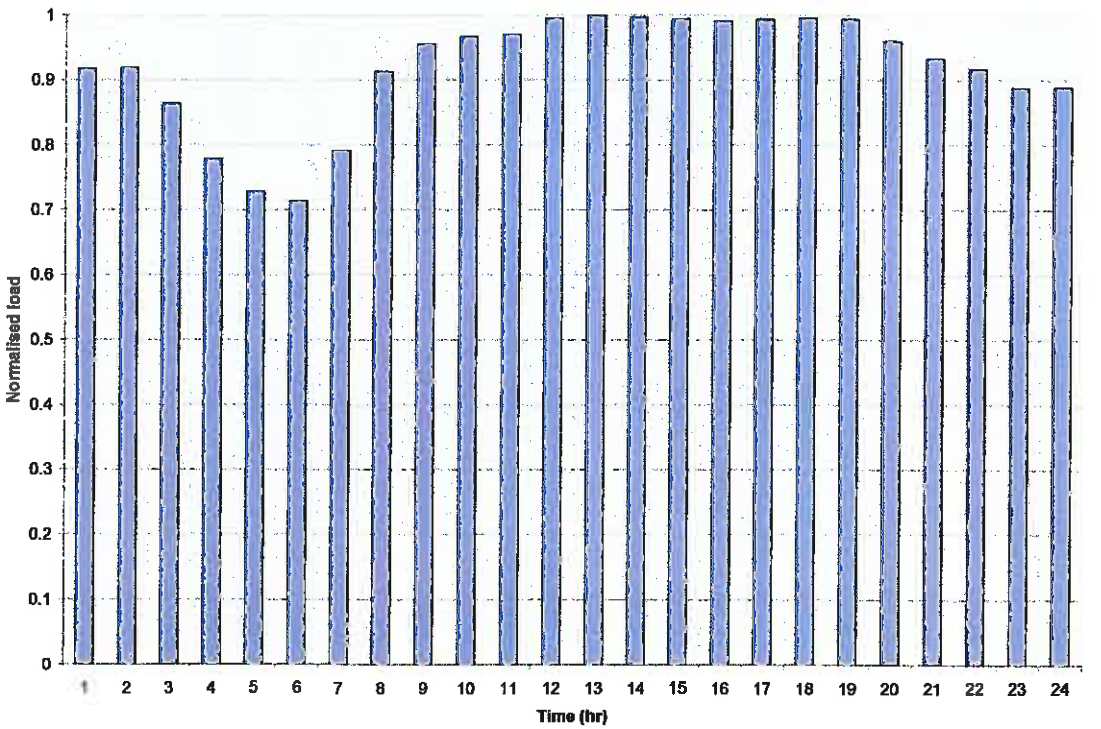

Motor vehicle sources were modelled in an Eulerian framework assuming a release height of 3 meters. Emissions were derived for the inner domain only from 1996 RTA measurements of VKT (RTA, 1996). These data account for all the major (and some of the minor roads within the area) as displayed in Figure 1. Emission rates were derived assuming a vehicle mix of 75% passenger vehicles, 10% light duty goods and 15% heavy

duty goods vehicles. The passenger vehicles were assumed to run on petrol. Light duty goods vehicles were assumed to be ⅔ petrol and ⅓ diesel, all heavy goods vehicles were assumed to be diesel. Diesel emission rates were derived from a CSIRO database of emissions measured as part of a study to develop an Australian National Environment Protection Measure (ANEPM) for diesel vehicles (Anyon et al, 2000). For the current study, the drive cycle was assumed to be equivalent to a highway cycle. Petrol emission rates were calculated from a power based model (Nyguen et al, 2000) using consistent highway drive cycles derived from the diesel study. Assumed characteristics for the petrol vehicles required for the power model are displayed in Table 3.

Table 3. Assumed vehicular properties

Vehicle type	Drag coefficient	Frontal area (m^2)	Mass (kg)	Engine capacity (L)
SI catalyst	0.35	2.0	1285	2.6
SI non catalyst	0.40	2.0	1200	2.5
Light duty	0.80	4.0	5250	4.2

Emissions from railway trains were also accounted for within the inner domain and were modelled in an Eulerian framework assuming a release height of 15 meters. In this case a train was assumed to consist of three 82 class locomotives operating at an average speed of 40 km/h. Average emissions were calculated from emission rates given by Lilley (1996) assuming the artificial throttle position profile displayed in Table 4.

Table 4. Artificial throttle position profile for trains operating within the inner domain.

Throttle notch position	Contribution (%)
Idle	10
1	7
2	10
3	12.5
4	15
5	15
6	12.5
7	10
8	8

The number of trains traveling the railway were dictated according to the basic artificial scheme displayed in Table 5. In this case, section 1 is the portion of the main railway (Northern line) south of Muswellbrook, section 2 is the portion of the Northern line north of Muswellbrook and section 3 is the remaining segment joining the Northern line from the west.

Table 5. Assumed hourly profile for train movements.

Hour	Section 1 (trains/h)	Section 2 (trains/h)	Section 3 (trains/h)
1	2.00	1.18	0.82
2	2.00	1.18	0.82
3	2.00	1.18	0.82
4	2.00	1.18	0.82
5	2.00	1.18	0.82
6	2.00	1.18	0.82
7	4.00	2.35	1.65
8	4.00	2.35	1.65
9	4.00	2.35	1.65
10	4.00	2.35	1.65
11	4.00	2.35	1.65
12	4.00	2.35	1.65
13	4.00	2.35	1.65
14	4.00	2.35	1.65
15	4.00	2.35	1.65
16	4.00	2.35	1.65
17	2.00	1.18	0.82
18	2.00	1.18	0.82
19	2.00	1.18	0.82
20	2.00	1.18	0.82
21	2.00	1.18	0.82
22	2.00	1.18	0.82
23	2.00	1.18	0.82
24	2.00	1.18	0.82
Total	68	40	28

Figure 5 displays a representation of proportion of the total daily CO_2 flux from each source within the inner domain for the spatially constant spontaneous combustion emission case. Clearly the power station emissions dominate and in this case account for 97% of the total emissions.

Figure 5: Proportion of daily CO_2 flux from sources within the inner domain

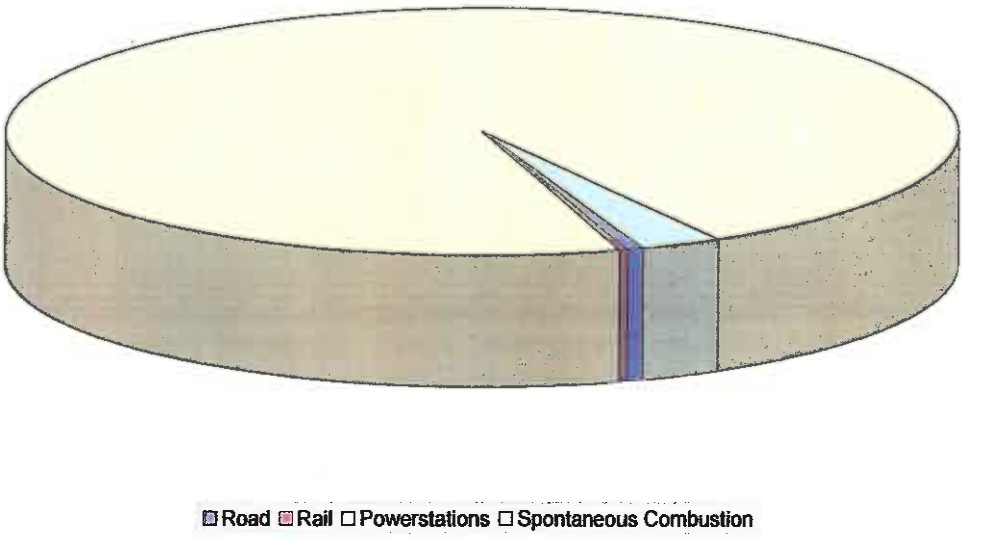

As a result of the data in Figure 5 it is important to consider the impact the other significant sources of CO_2 may have on a monitoring site specifically deployed to measure emissions from spontaneous combustion. This is considered in the following Section.

3. RESULTS

3.1 Spatially constant emission rate

Figures 6, 7 and 8 show the maximum, 9th highest and annual average CO_2 concentrations within the inner domain for all sources. Note that the 9th highest value is often used in air quality modelling as it avoids the extreme events associated with the largest value. (The 9th highest value corresponds to the 99.9 percentile of the 8760 hours in a year). Note also that in this document the CO_2 concentrations refer to values above ambient background.

From the data in Figure 6 it can be seen that the range of maximum values produced by the spontaneous combustion and power station sources are similar, and both considerably larger than traffic and rail contributions. The magnitude of CO_2 concentrations from spontaneous combustion sources is however largest when considering the 9th highest and annual average data. This is because of the different nature of the two sources. The spontaneous combustion source is a distributed area source whereas the power stations correspond to elevated point sources. The maximum ground level concentrations from the power stations correspond to meteorological conditions when the plumes touch down close to the source. On the other hand the maximum values from the surface sources will arise from light wind conditions and very stable air. Also apparent from the annual averages (Figure 8) is the predominance of NW and SE flows within the Valley.

The above trends are shown in more detail in Figures 9 and 10, which display the contribution of each source to the annual average CO_2, and range in CO_2 concentrations as a function of time of day, respectively. These data relate to time series extracted at Point A (see Figure 1). It is clear that the locomotive and traffic generated CO_2 concentrations are small in comparison to the power station and spontaneous combustions sources for both the average and range in CO_2 concentrations. While the range is similar for both the spontaneous combustion and power station sources, the average value is larger for the spontaneous combustion source. Further it is apparent that the ground level spontaneous combustion sources dominate between the hours of 9 p.m. to 8a.m. and the power station sources dominate between 11a.m. and 7p.m. These trends are the result of the interaction of the plumes from the two sources and the atmospheric boundary layer. For elevated plumes in stable nighttime conditions the plumes spread very little in the vertical and horizontal planes and are essentially decoupled from the surface and have no impact at the surface. Ground level plumes on the other hand are constrained by the stable air and also spread very little in the vertical and horizontal planes giving rise to elevated concentrations at the ground. As the ground heats, after the sun rises, the atmosphere starts to mix and typically around mid morning mixing reaches the elevated plumes and brings them to ground resulting in elevated concentrations from the power station plumes. The same mixing process also acts to spread the surface plumes in both the vertical and horizontal planes resulting in reduced concentrations during the middle of

Figure 6. Maximum yearly CO_2 GLC for a constant emission source

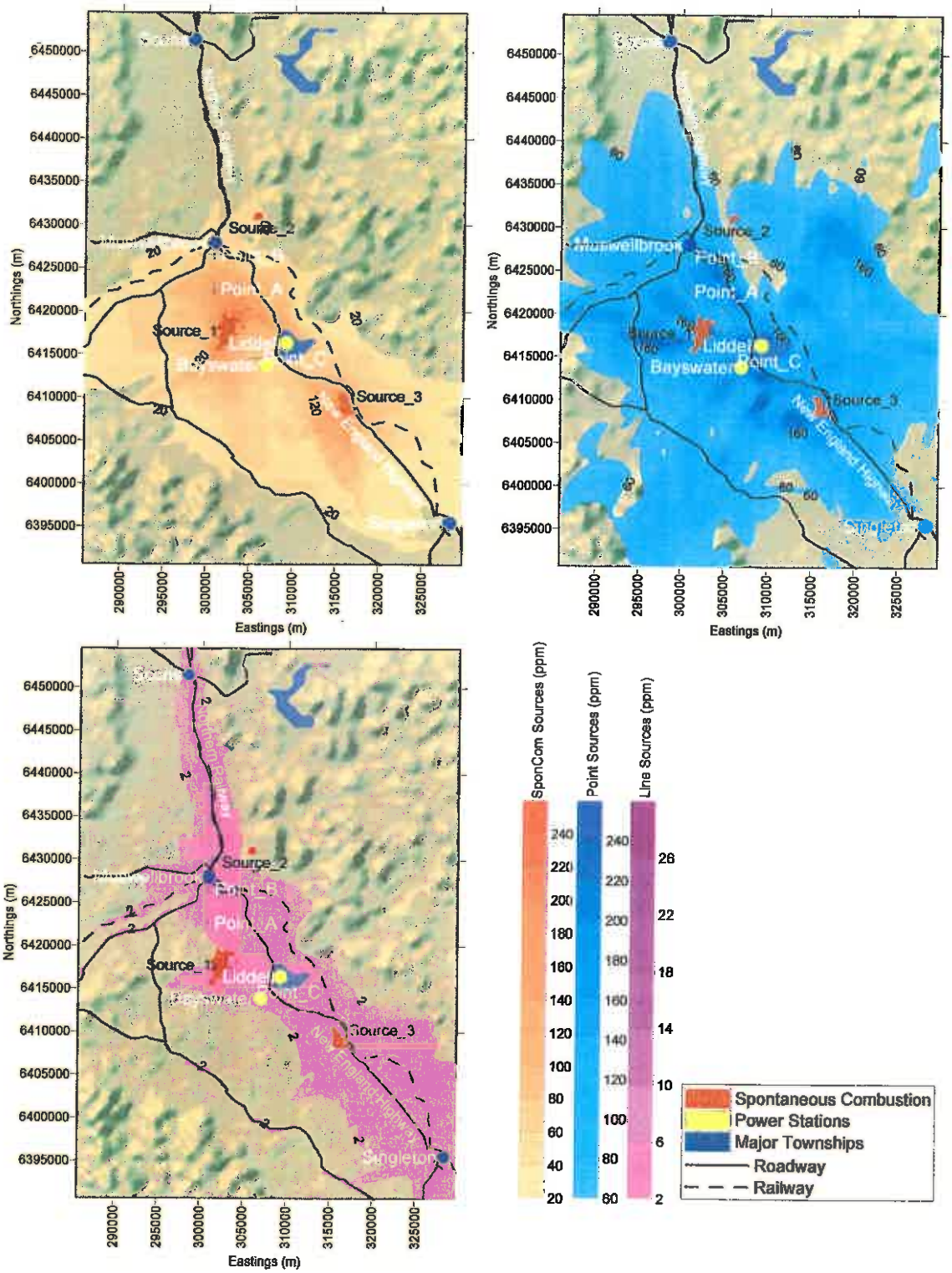

Figure 7. 9th highest yearly CO_2 GLC for a constant emission source

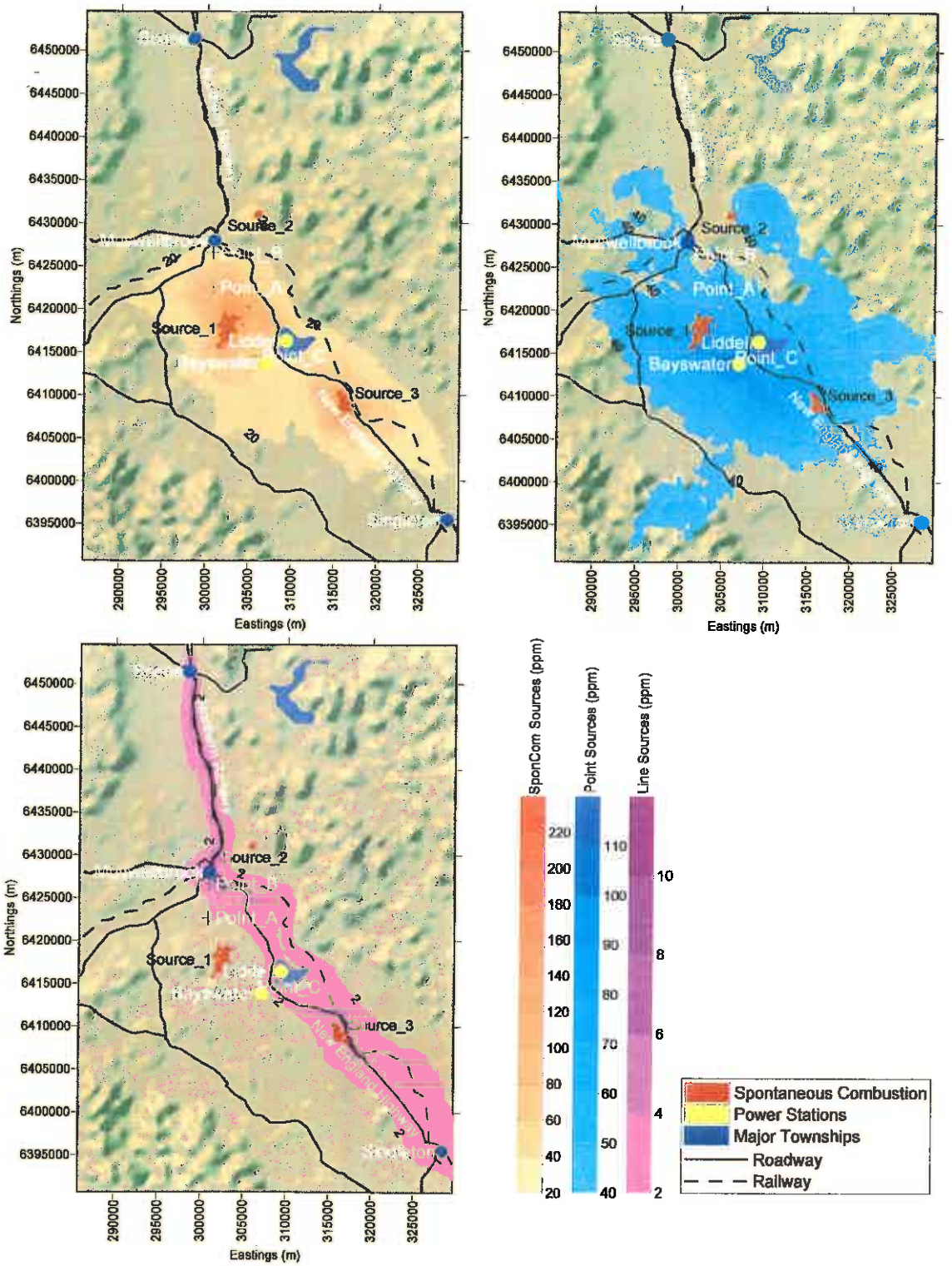

Figure 8. Annual average CO_2 GLC for a constant emission source

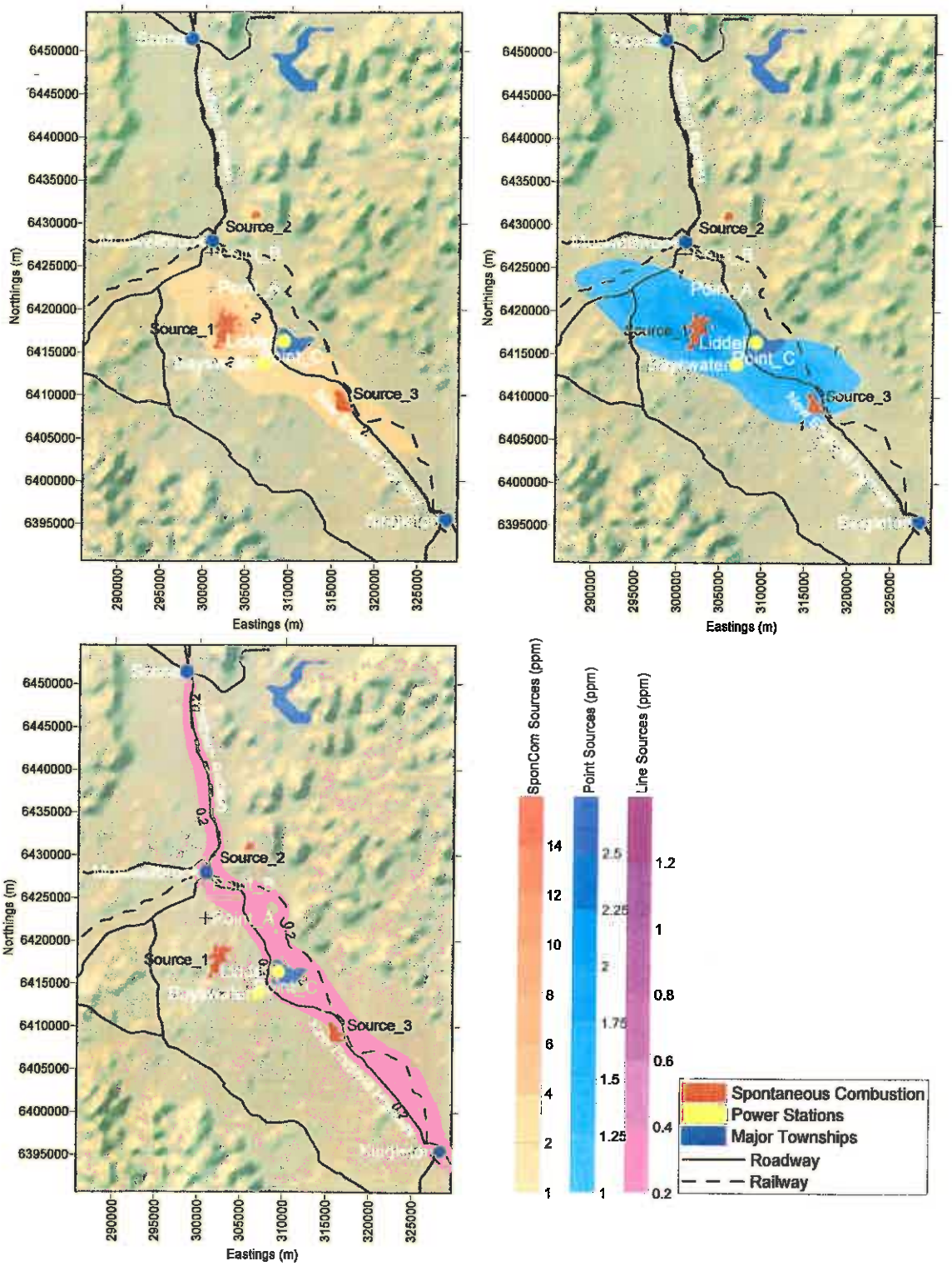

Figure 9. Average CO_2 concentrations plotted as a function of time of day for point A for a spatially constant emission source

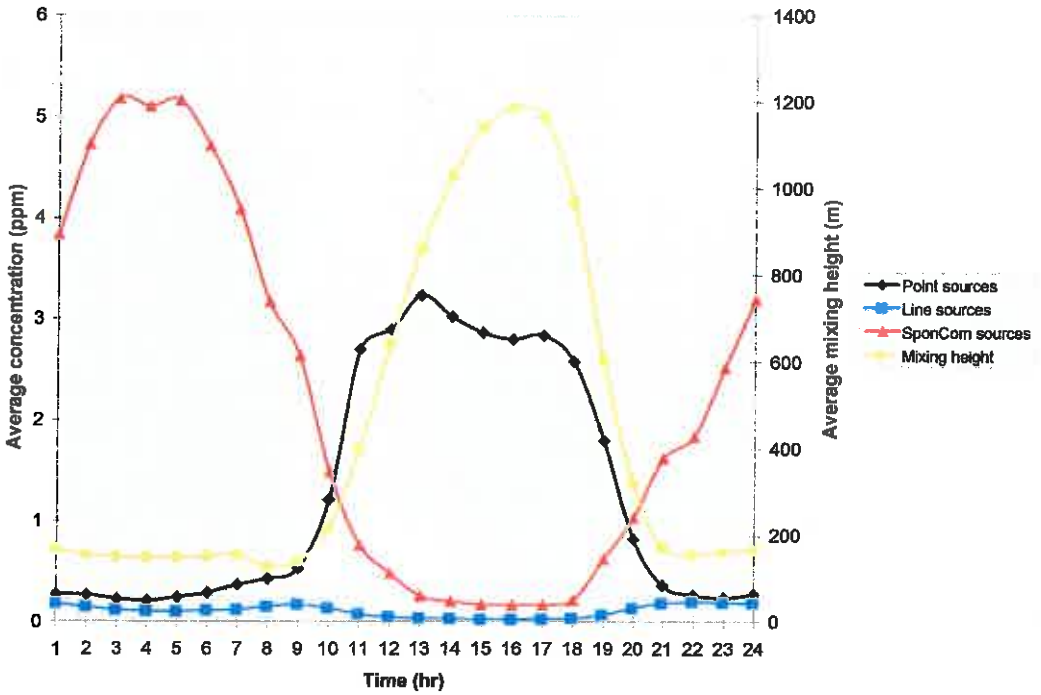

Figure 10. CO_2 concentration range plotted as a function of time of day for point A for a spatially constant emission source

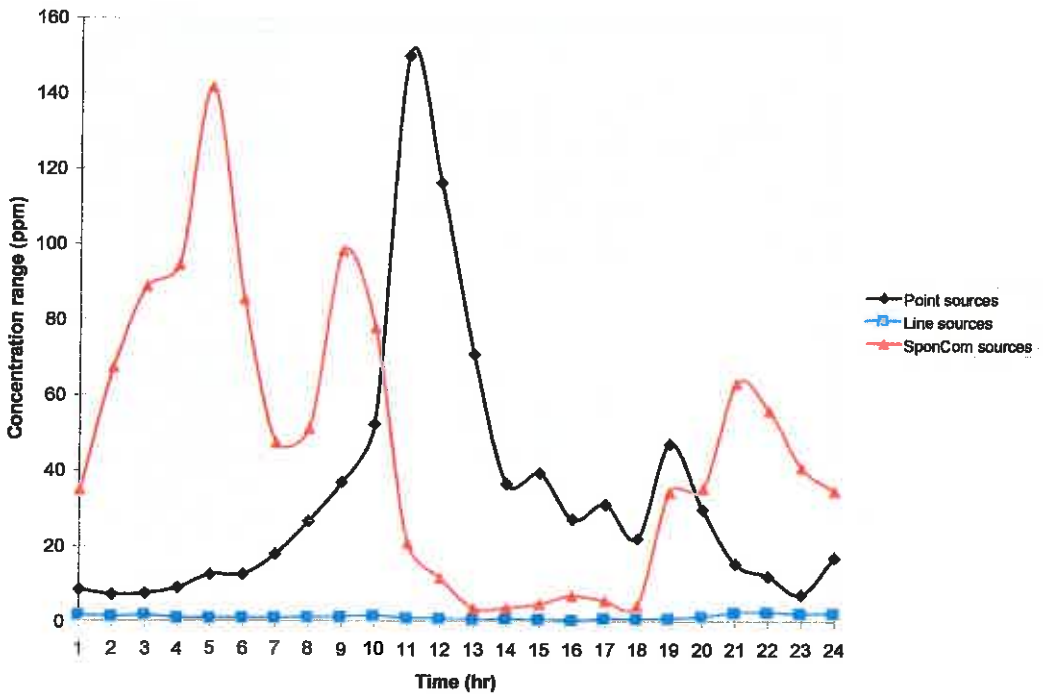

the day period. The calculated mixing height, is also shown for purposes of illustration in Figure 9.

While the data in Figures 8 and 9 are indicative of the results obtained they also depend on the location of the receptor site. In fact Points A and C were chosen on the basis of receiving a greater proportion of mass from Source 1. Point B was selected as a comparison as it was positioned just outside the zone of greatest influence and was possibly compromised by other spontaneous combustion and external sources.

3.2 Hotspot sensitivity.

In order to examine the effect of high spatial variation within the spontaneous combustion area source, eight scenarios were modelled for a one-month period (February) with hotspot areas as shown in Figure 2. Initially, only spontaneous combustion sources were considered. Also the data examined at Points A and B have been restricted to a window of 120° to 170° and Point C data filtered between 280° to 330°. (Note the wind direction filtering is a further attempt to restrict the data examined to periods when the wind direction was from the spontaneous combustion sources heading toward the monitoring sites). Further, in accordance with results displayed in Figures 9 and 10, the data have only been considered for the hours from 9p.m. to 8a.m.

Figure 11 shows the maximum 1 hourly differences for each month (i.e. hotspot case – basecase) where the base case corresponds to the constant emission rate described in Section 3.1. The results show that the maximum hourly differences resulting from the hotspot additions scenarios. While there are large differences close to the source these fall off rapidly with distance.

Figure 12 shows the monthly average differences between the hotspot additions and the base case.

Figure 11. Maximum monthly difference (hotspot case – basecase).

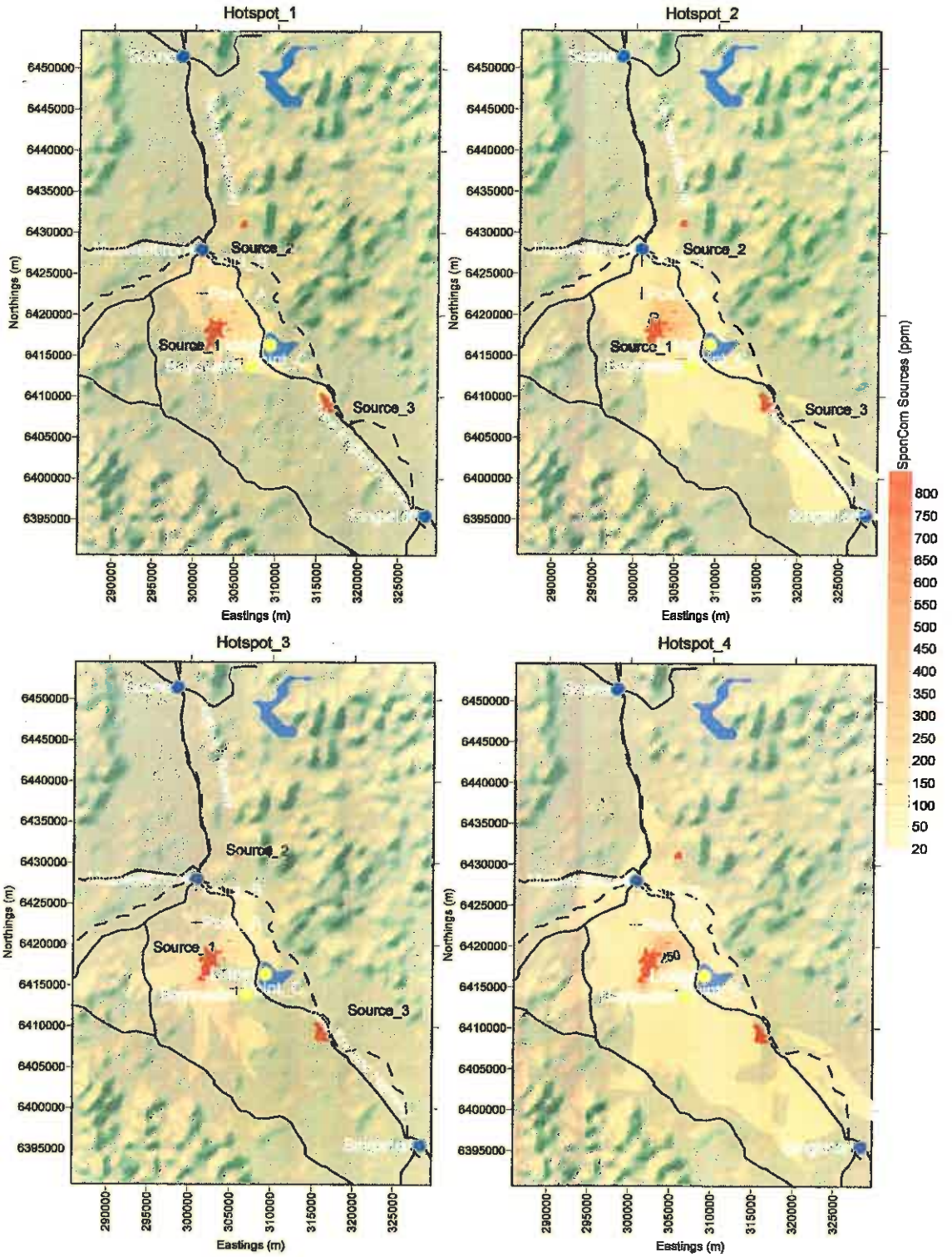

Figure 11 (cont). Maximum monthly difference (hotspot case – basecase).

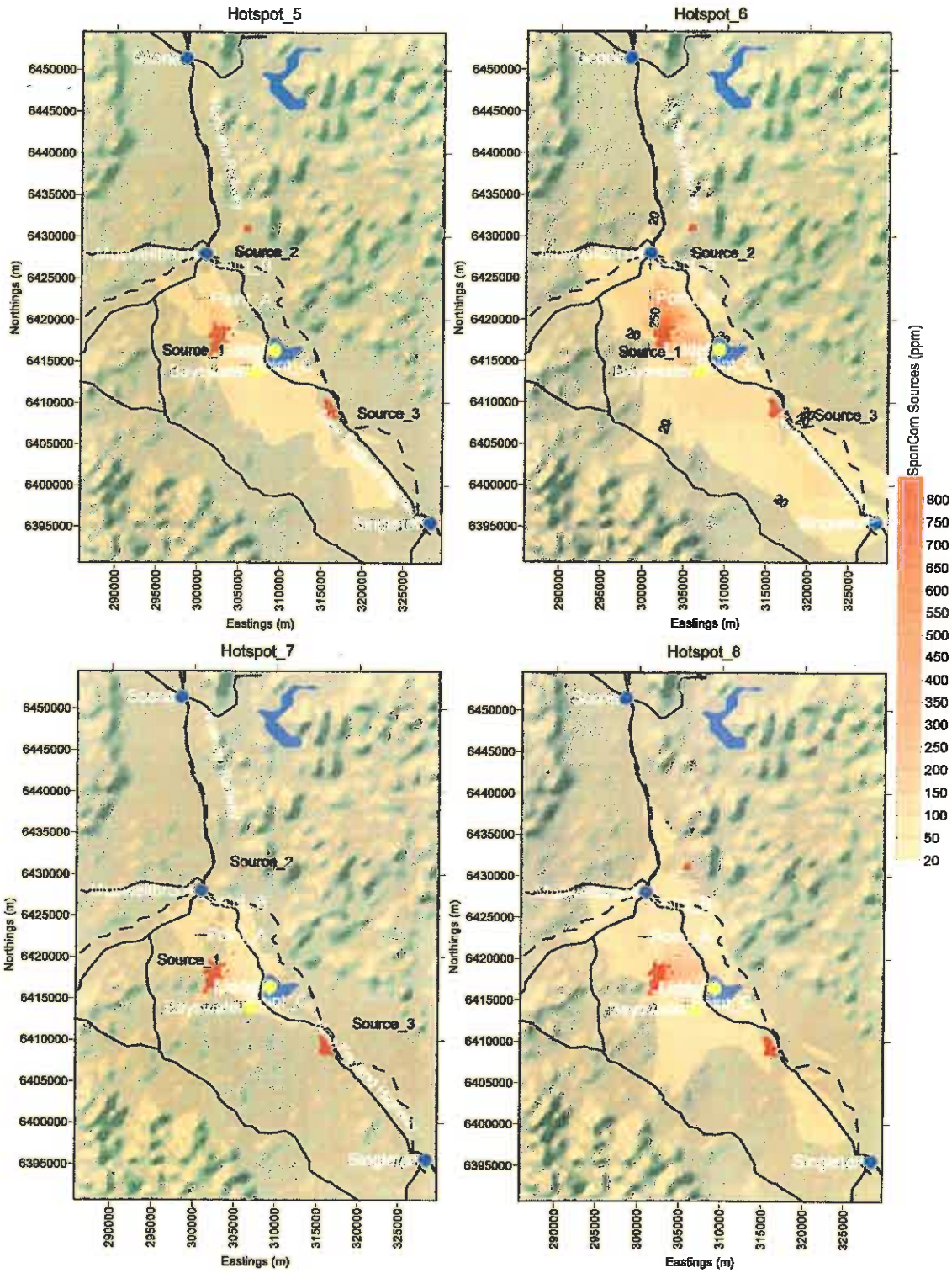

Figure 12. Average monthly difference (hotspot case – basecase).

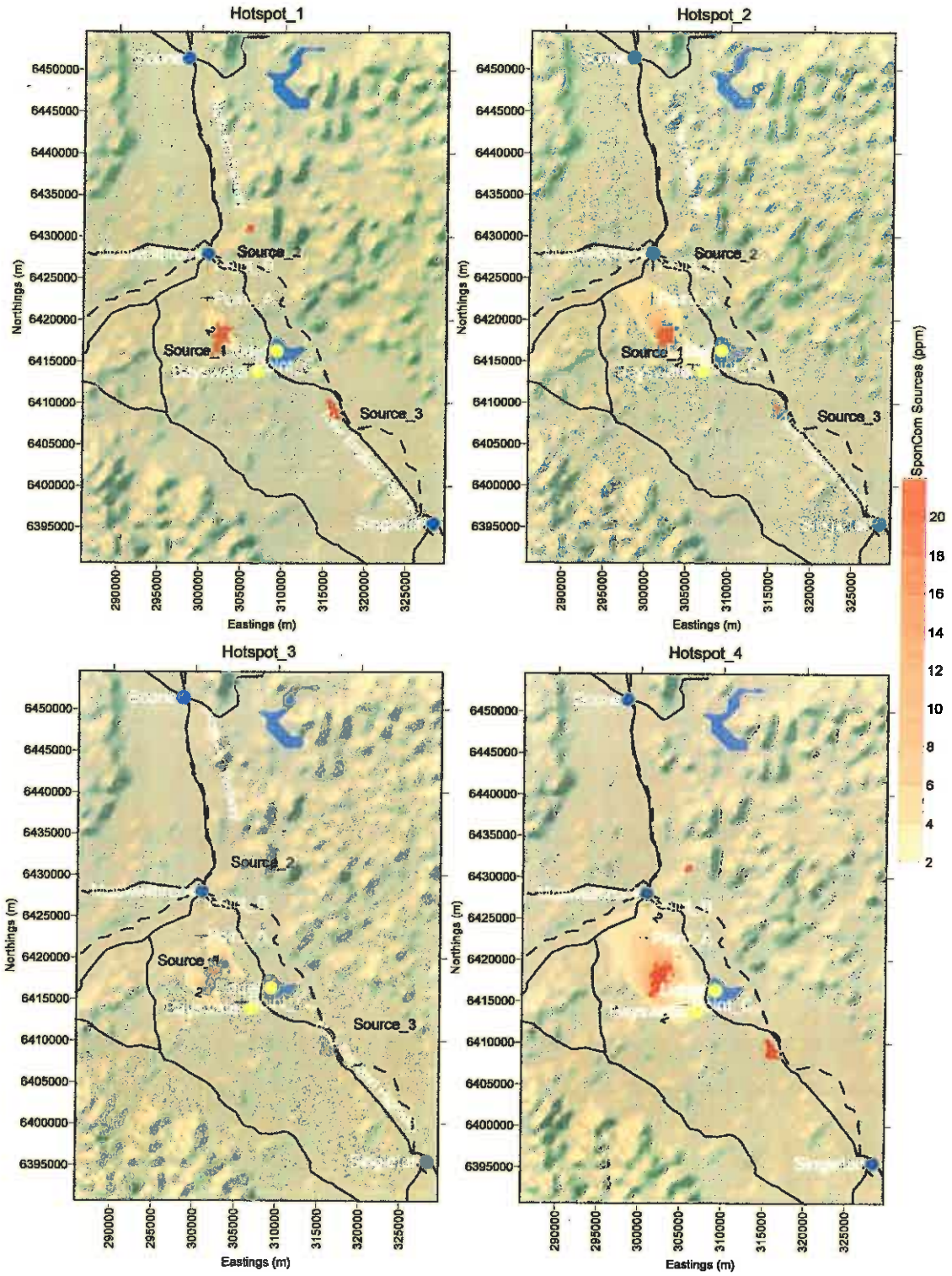

Figure 12 (cont). Average monthly difference (hotspot case – basecase).

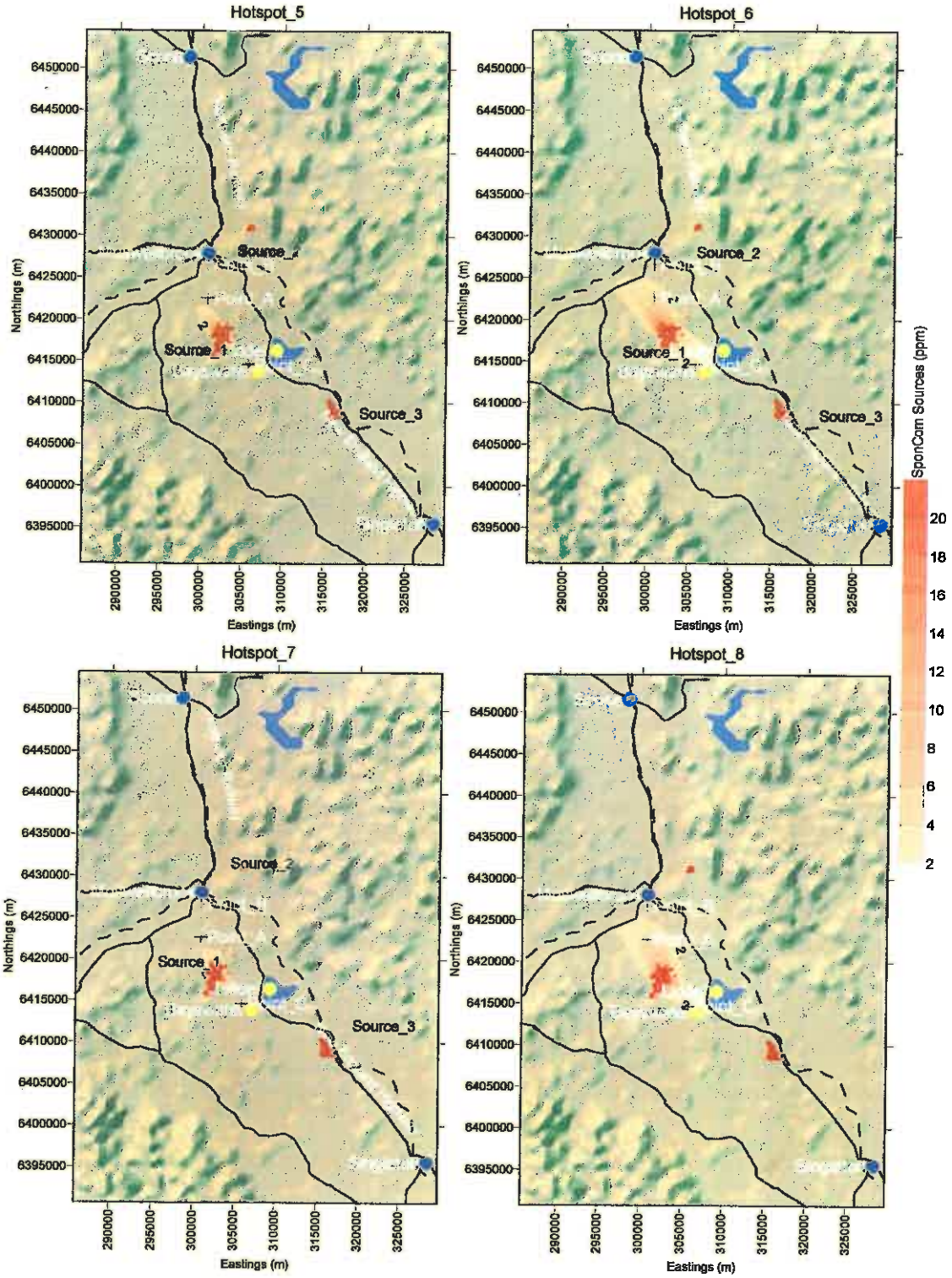

Figure 12 (cont). Average monthly difference (hotspot case – basecase).

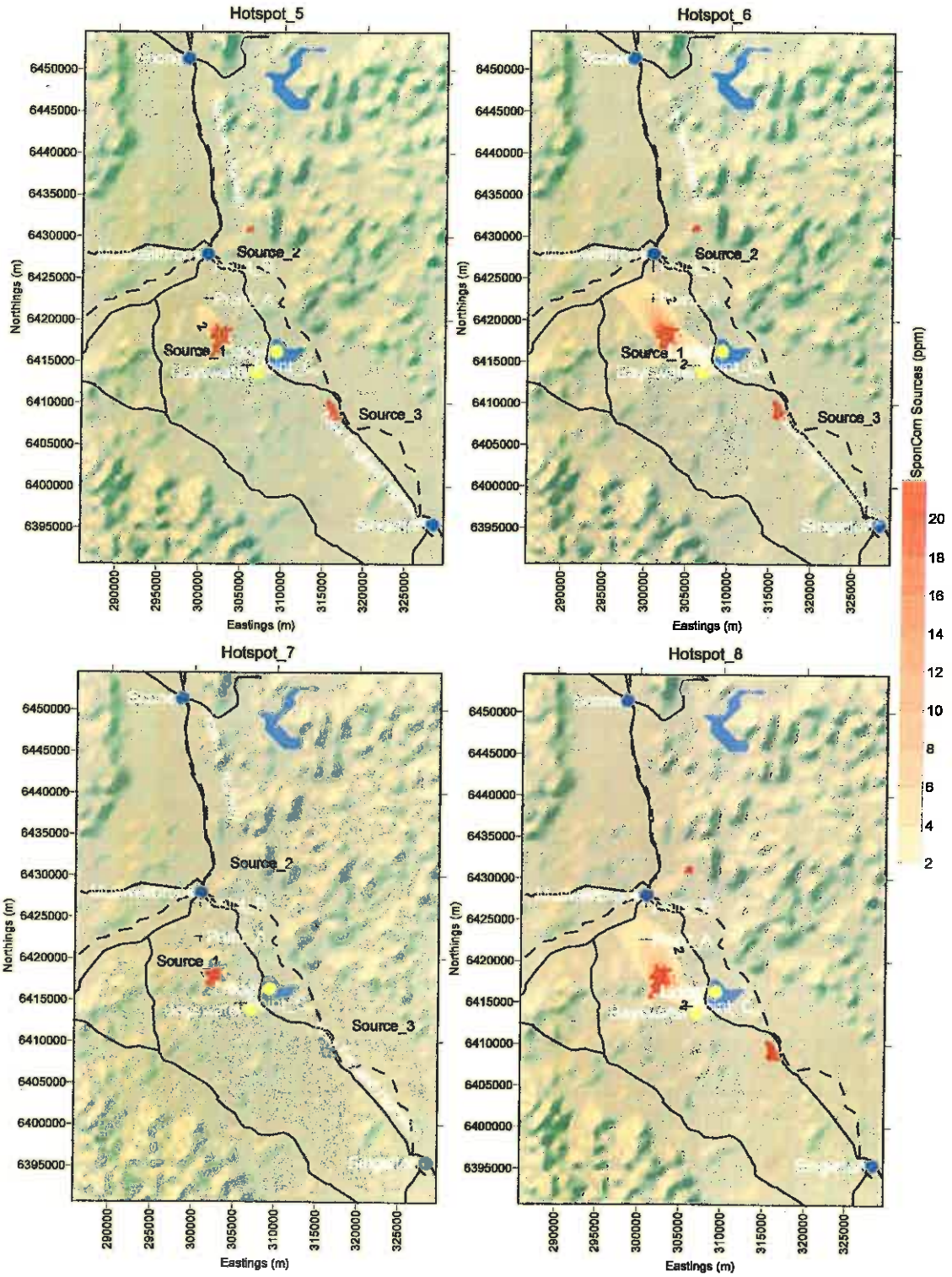

In the current work and in the absence of a concentration time series that could be used for the inverse calculation we have carried out a number of numerical investigations to assess the sensitivity of a simple method to determine the emissions from spontaneous combustion. The method is based on the use of the annual average and is intended to illustrate some of the issues that would be considered in a full air quality based approach to the estimation of emissions from an area source.

As discussed in Section 2.1 the concentration at any point downwind of a constant emission source can be considered simply as, $\chi_t = f_t Q$, where the function f_t contains all relevant information concerning atmospheric transport, dilution and diffusion.

At any point downwind of a source, say at Point A and for a constant emission rate of Q_1 and dropping the subscript 't', the annual average is defined as

$$\overline{\chi_{A_1}} = \int \chi_{A_1} dt / \int dt = Q_1 \int f_A dt / \int dt$$

where the integrals are taken over a 1 year period.

For a source of strength Q_2 from the same location, a similar expression can be written for the time average at Point A ie $\overline{\chi_{A_2}}$. Consequently for a single source the ratio of the concentrations at Point A for the two sources strengths is

$$\overline{\chi_{A_1}} / \overline{\chi_{A_2}} = Q_1 / Q_2$$

Tables 6a and 6b display the calculated normalised source strength and gross error estimates for each of the hotspot scenarios for points A, B and C. These estimates have been formed from the above expression as

$$\chi_h / \chi_{bc} = \int Q_h f dt / Q_{bc} \int f dt = \overline{Q}_h / Q_{bc}$$

where in the current work $\overline{Q}_h$ has been taken to represent the average emission rate for the source. (The subscripts *'h'* and *'bc'* refer to 'hotspot' and 'base case' respectively).

Table 6a. Normalised hotspot scenario source strengths.

	Actual	Point A	Point B	Point C
Hotspot_1	1.30	1.26	1.13	1.18
Hotspot_2	1.90	1.83	1.45	1.93
Hotspot_3	1.60	1.75	1.92	1.41
Hotspot_4	2.50	2.51	2.47	2.36
Hotspot_5	1.30	1.30	1.08	1.21
Hotspot_6	1.90	2.00	1.45	1.81
Hotspot_7	1.30	1.31	1.36	1.29
Hotspot_8	1.90	1.84	1.87	1.93

Table 6b. Gross errors (%) for each hotspot scenario.

	Point A	Point B	Point C
Hotspot_1	-3.1	-13.1	-9.2
Hotspot_2	-3.7	-23.7	1.6
Hotspot_3	9.4	20.0	-11.9
Hotspot_4	0.4	-1.2	-5.6
Hotspot_5	0.0	-16.9	-6.9
Hotspot_6	5.3	-23.7	-4.7
Hotspot_7	0.8	4.6	-0.8
Hotspot_8	-3.2	-1.6	1.6

Generally, the total source strength was predicted acceptably well particularly for points A and C. The predictions for Point B are strongly influenced by the relatively weak impact the spontaneous combustion sources have at Point B. (These results have also been affected by truncation errors in TAPM). However even then the maximum absolute error is still only ~24% for hotspot scenarios 2 and 6. As these results are formed using concentrations derived from only spontaneous combustion sources they represent the inherent error in the above simple methodology for these cases, which arises from the method by which the area source emission has been approximated.

It is possible to obtain far greater resolution of the area source by the use of a local intense plume model as described by Lehning et al (1994). The plume model would be used in conjunction with TAPM and with field data. This is the approach that would be pursued in further work. However, the simple approach taken above, in the absence of field and monitoring data is also instructive.

3.3 Thermally derived emissions

Further effects from spatial variation were investigated using an emission profile for Source 1 estimated from thermography. In this case, a year long run was performed. Figure 13 displays the maximum and maximum difference (thermal case – basecase) CO_2 concentrations from spontaneous combustion sources.

Figure 13. Maximum CO_2 and maximum CO_2 difference (thermal case –basecase).

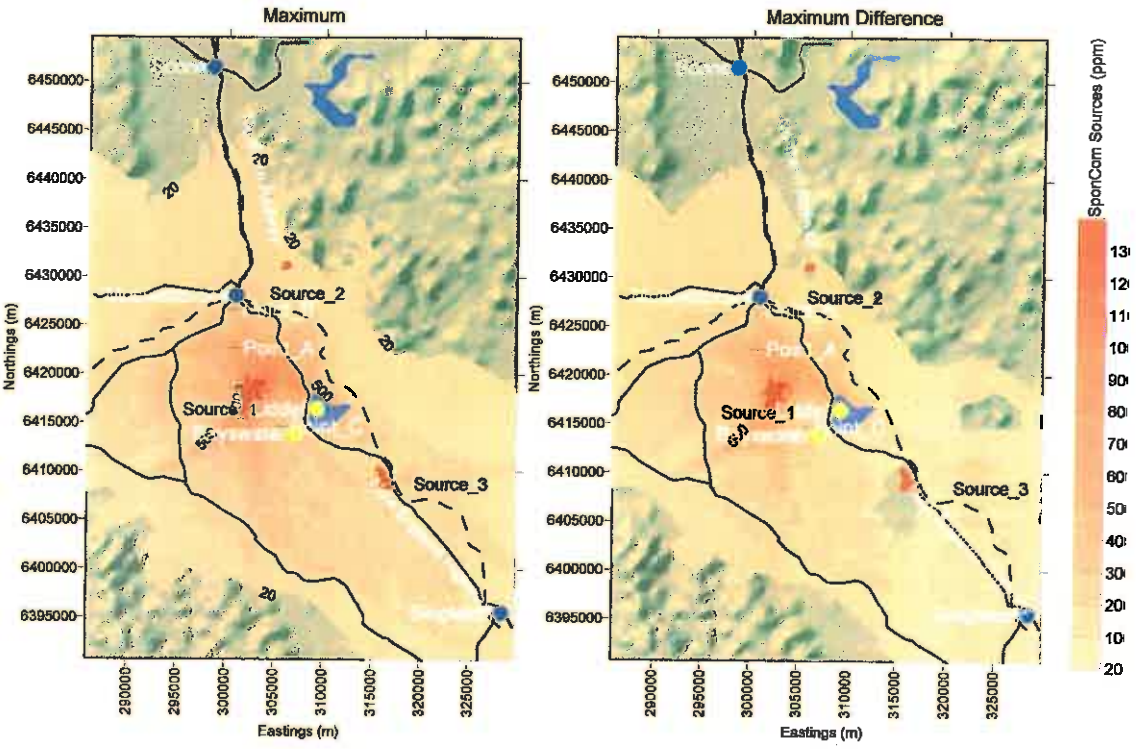

Likewise, Figure 14 provides results for the annual average. The figures indicate that there is considerable variation in emission intensity in comparison with the basecase and some spatial variation particularly north and south of Source 1.

Figure 14. Annual average CO_2 and annual average CO_2 difference (thermal case – basecase).

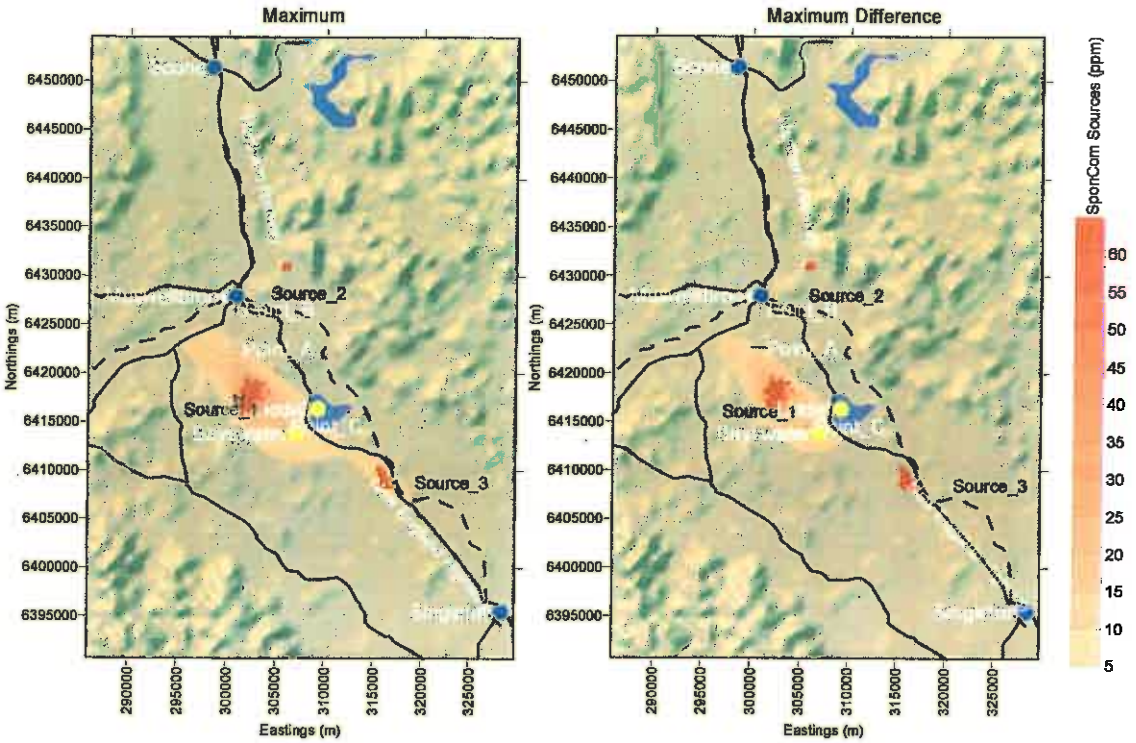

Tables 7a and 7b, display the calculated source strength and gross errors for the thermographic based emissions. The error estimates are higher for this more complicated scenario than those displayed in Tables 6a and 6b for the monthly hotspot scenarios. For instance the estimates for Points A and C vary for the annual results from and underestimation by 17% at Point A to an overestimation of ~16% at Point C. The large errors at point B are indicative of the point being too far from the source. This increases the errors associated with model uncertainty and truncation errors from the TAPM ground level concentration files.

Table 7b shows that there is considerable seasonal variation due primarily to the change in dominant wind patterns, affecting both the relative spread and the number of recorded signals greater than zero.

Table 7a. Normalised thermographic based scenario source strengths

	Actual	Point A	Point B	Point C
Yearly	4.25	3.52	2.42	4.92
Summer	4.25	3.46	2.02	5.01
Autumn	4.25	3.69	2.37	5.04
Winter	4.25	3.30	2.46	4.85
Spring	4.25	3.44	2.52	4.66
February only	4.25	3.79	2.66	4.51

Table 7b. Gross errors (%) for the thermographic based scenario

	Point A	Point B	Point C
Yearly	-17.2	-43.1	15.8
Summer	-18.6	-52.5	17.9
Autumn	-13.2	-44.2	18.6
Winter	-22.4	-42.1	14.1
Spring	-19.1	-40.7	9.6
February only	-10.8	-37.4	6.1

In an attempt to examine the impact of noise in the data, a perturbation study was carried out. This was done by adding a random error of either ± 1 ppm or ± 3 ppm to the spontaneous combustion derived concentrations. The mean and standard deviations derived from 20 realisations are shown in Table 8. The values of ±1 ppm and ±3 ppm were chosen to represent the general noise associated with standard CO_2 measuring equipment. The data show that while the mean values are unchanged for the random errors there is a change in the deviation from the mean, as expected. Generally the method is insensitive to the induced error particularly at points A and C. These results are not surprising given the perturbation is small in comparison to the arithmetic mean (for the selected time period and wind directions) of 29.7 ppm and 45.6 ppm for points A and C and similar in magnitude to the value of 3.29 ppm for point B.

Table 8. Perturbation results for yearly data

	Point A	Point B	Point C
± 1 PPM			
Mean	3.52	2.44	4.92
Standard Dev	0.005	0.014	0.005
± 3 PPM			
Mean	3.52	2.44	4.92
Standard Dev	0.009	0.047	0.007

Finally, Tables 9a and 9b provide source strength and gross error results using the concentrations for emissions derived from all sources.

Table 9a. Normalised thermographic based scenario source strengths including all sources

	Actual	Point A	Point B	Point C
Yearly	4.25	3.58	2.87	4.96
Summer	4.25	3.57	2.42	5.09
Autumn	4.25	3.74	2.76	5.05
Winter	4.25	3.36	3.26	4.92
Spring	4.25	3.52	3.16	4.70

Table 9b. Gross errors (%) for the thermographic based scenario including all sources

	Point A	Point B	Point C
Yearly	-15.8	-32.5	16.7
Summer	-16.0	-43.1	19.8
Autumn	-12.0	-35.1	18.8
Winter	-20.9	-23.3	15.8
Spring	-17.2	-25.6	10.6

These results are similar to those derived using only spontaneous combustion sources. Point B is somewhat of an exception with a moderate improvement due to its proximity to road and railways. The results indicate that by careful placement of a monitoring site and with appropriate spatial and temporal filtering, the effect of other sources may be essentially eliminated, reducing the need for specialised filtering to remove them.

While the methodology derived in this study indicates comparisons can be drawn without adjusting the observational data, it is imperative that an estimate of other sources within the vicinity of the spontaneous combustion sources be developed. This is important to justify extending the methodology to other regions and in choosing appropriate monitoring locations.

3.3 Further Considerations

The method presented above relies upon describing the dilution function f well. In the current study, $f_{(obs)}$ and $f_{(model)}$ are identical. When using real world data this will not be the case due to the inability of models to perfectly forecast the weather and air quality. Restricting comparisons to occasions when the observed meteorological fields match the modelled meteorology within selected bounds will assist in removing errors associated with model performance.

In addition to good quality CO_2 monitoring data, access to micrometeorological data from the existing tower in the Upper Hunter would allow periods for study to be chosen so that the accuracy of the model predictions could be greatly increased.

However, in addition to the monitoring data and numerical modelling, greater accuracy would result from a concurrent program of ground based traversing coupled to the micrometeorological data and the plume modelling. A simpler plume model used in conjunction with the air quality model TAPM, and the extra field data would provide the basis for a robust methodology to estimate greenhouse gas emission from spontaneous combustion. This approach forms the basis of the next phase of this work which is seeking funding from ACARP.

4. CONCLUSION

An investigation of CO_2 sources in the Upper Hunter Valley has shown that spontaneous combustion and power stations can give rise to significant concentrations at ground level. However the impact of the power stations emissions are most pronounced during the day time hours while the impact of the spontaneous combustion emissions are most pronounced during the night time. This is because the former are elevated while the latter are ground level sources. This suggests that concentration measurements should focus on data during the night time period. While the emissions from road traffic and rail are significant their ground level concentration signature is not as pronounced as for the other two major sources.

Consideration of results of the air quality modelling suggests that monitoring sites for the inverse modelling should be sited such that;

- The location point should be sufficiently close to the spontaneous combustion sources to enable a large measurable signal.
- The site should be chosen on the basis of meteorology to best capture the likely CO_2 spontaneous combustion signal
- The sites should be chosen to minimise the influence of other sources.

In order to examine some of the issues that would need to be taken into account in using air quality methods, concentrations were predicted for three chosen locations and examined in greater detail. The predicted concentration time series were used as surrogates for measured data and a simple ratio method used to produce results which highlighted the uncertainties associated with this approach.

In addition to these inherent uncertainties there will also be those due to the non ideal nature of the data and the fact that the air quality model still represents an approximation to reality. Supplementation of the CO_2 concentration data with other micrometeorological data would constrain the data and reduce the uncertainty. In addition concurrent ground based field measurements of CO_2 traverses across the plume coupled with the micrometeorological data and detailed plume modelling would provide the basis for a robust methodology to estimate greenhouse gas emissions from spontaneous combustion.

5. REFERENCES

Anyon P, Brown S, Pattison D, Beville-Anderson J, Walls G and Mowle M (2000). In service emissions performance – phase 2: Vehicle Testing. *Final report to National Environment Protection Council*, Adelaide, SA, Australia.

van Aardene JA, Builtjes PJH, Hordijk L, Kroeze C and Pulles MPJ (2002). Using wind-direction-dependent differences between model calculations and field measurements as indicator for the inaccuracy of emission inventories. *Atmospheric Environment*, **36,** 1195-1204

Azzi M. Johnson G.M. and Cope M. (1992) An introduction to the generic reaction set photochemical smog mechanism. *In Proc. 11th Clean Air Conference and 4th Regional IUAPPA Conf., Brisbane Australia.*

Carras JN, Day S, Saghafi A and Williams DJ (2000) Measurement of greenhouse gas emissions from spontaneous combustion in open cut coal mining. ACARP C8059, pp46.

Carras JN, Day S, Szemes F, Watson JA and Williams DJ (2002) An evaluation of the use of airborne infra-red thermography as a method for monitoring spontaneous combustion and greenhouse gas emissions. ACARP C9062, pp41.

ESSA (2001). Electricity Australia 2001, pp72. Electricity supply association of Australia, Sydney, NSW, Australia.

Hurley, P. (1998) Model any region for EIAs on a PC. *Proc. 11th International Clean Air Conference of CASANZ*, Melbourne, 18-22 October 1998.

Lehning M, Chang DPY, Shonnard DR and Bell RL (1994) An inversion algorithm for determining area-source emissions from downwind concentration measurements. *Journal of Air and Waste Management Association,* **44,** 1204-1213.

Lilley W (1996). Quantification and dispersion modelling of diesel locomotive emissions. Unpublished Honours Thesis, Newcastle University, NSW, Australia.

Manins PC, Carras JN and Williams DJ (1992). Plume rise from multiple stacks, *Clean Air*, **26**, 65-68.

Mulholland M and Seinfeld JH (1995). Inverse air pollution modelling of urban scale carbon monoxide emissions. *Atmospheric Environment*, **29,** 497-516.

NGGI (1996). Methodology for the estimation of greenhouse gas emissions and sinks. Supplement to workbooks 1.0-8.0, pp249. National greenhouse gas inventory committee, Canberra, ACT, Australia.

Nyugen N, Lilley W and William DJ (2000). Development of a technique for estimating traffic emission and fuel consumption from SCATS road networks. *Proc. 15th International Clean Air Conference of CASANZ*, Sydney, 26-30 November 2000.

RTA (1996). Traffic volume data for northern region 1996, pp297. Roads and Traffic Authority, Sydney, NSW, Australia.